How Far is Far Enough?: The Fetch Requirements for Micrometeorological Measurement of Surface Fluxes

T. W. HORST AND J. C. WEIL*

National Center for Atmospheric Research,† Boulder, Colorado

(Manuscript received 26 March 1993, in final form 27 December 1993)

ABSTRACT

Recent model estimates of the flux footprint are used to examine the fetch requirements for accurate micrometeorological measurement of surface fluxes of passive, conservative scalars within the surface flux layer. The required fetch is quantified by specifying an acceptable ratio of the measured flux to the local surface flux. When normalized by the measurement height z_m, the fetch is found to be a strong function of atmospheric stability as quantified by z_m/L, where L is the Obukhov length, and a weaker function of the normalized measurement height z_m/z_0, where z_0 is the roughness length. Stable conditions are found to require a much greater fetch than do unstable conditions, and the fetch required for even moderately stable conditions is for many situations considerably greater than 100 times the measurement height.

1. Introduction

Surface fluxes are commonly inferred from vertical fluxes that are measured by micrometeorological techniques such as eddy correlation or eddy accumulation. Because these techniques require measurements to be made at some height above the surface, the inferred surface flux measurement is effectively averaged over an extended surface area upwind of the sensor location that is quantified by the flux "footprint." However, if surface flux inhomogeneities within the measurement footprint cause horizontal advection and thus vertical flux divergence, the measured flux will not equal the surface flux of interest. This paper focuses on the relationship between the vertical flux of a passive, conservative scalar—for example, carbon dioxide or methane—measured at some height above the surface and the upwind spatial distribution of the corresponding surface emission (or deposition) flux. In particular, we examine the upwind extent of homogeneous fetch that is necessary for a micrometeorological flux measurement to be within specified limits of the local surface flux. This study is based on recent analytic and numerical estimates of the flux footprint for the surface flux layer (Horst and Weil 1992, hereafter HW).

Schuepp et al. (1990) use the term "footprint" for the contribution, per unit surface flux, of each unit element of the upwind surface area to a measured vertical flux. This is illustrated in Fig. 1 for a tower-based flux measurement. The plan view shows isopleths of the footprint function for a wind blowing from right to left, and the profile view shows the crosswind-integrated flux footprint. The footprint has its maximum directly upwind of the measurement location, decreases slowly upwind of the maximum, and decreases very rapidly downwind of the maximum. The flux footprint f relates the vertical turbulent flux measured at height z_m, $F_m(x, y, z = z_m)$, to the spatial distribution of surface fluxes, $F_0(x, y, z = 0)$; that is,

$$F_m(x, y, z_m) = \int_{-\infty}^{\infty} \int_{-\infty}^{x} F_0(x', y', z' = 0) \times f(x - x', y - y', z_m)dx'dy'. \quad (1)$$

The measured flux is the integral of the contributions from all upwind surface elements; the flux footprint is the relative weight given to each elemental surface flux. It is assumed here that the turbulent flow field is horizontally homogeneous, and therefore the footprint depends only on the separation between the measurement point and the site of each elemental surface flux. The separation in the streamwise direction is $x - x'$, with the wind blowing in the positive x direction, and the separation in the crosswind direction is $y - y'$. As will be seen in section 4, the integral of f over the entire upwind surface is equal to unity in the surface (or constant) flux layer, so that for a horizontally homogeneous surface flux, that is F_0 is constant, Eq. (1) gives $F_m = F_0$ as expected.

* Permanent affiliation: Cooperative Institute for Research in Environmental Sciences, University of Colorado, Boulder, Colorado.

† The National Center for Atmospheric Research is sponsored by the National Science Foundation.

Corresponding author address: Dr. Thomas W. Horst, NCAR/ATD, P.O. Box 3000, Boulder, CO 80307-3000.

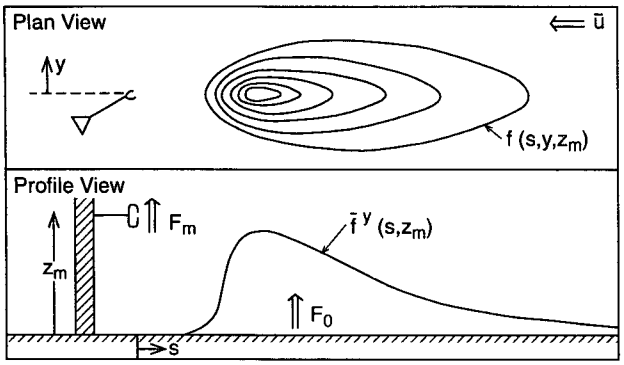

FIG. 1. Plan and profile sketches of the flux footprint function f for a tower-based flux measurement.

The flux footprint definition embodied in (1) is based on the principle of superposition, which states that fields governed by linear equations can be determined by summing any number of individual solutions to the governing equation, provided that the sum of the boundary conditions for the individual solutions satisfies the boundary condition for the situation of interest. The concentration of an atmospheric constituent is determined by an advection–diffusion equation, which is linear provided the constituent does not have nonlinear sources or sinks, for example, a nonlinear chemical reaction. Correspondingly, the equation for the vertical turbulent flux of the constituent is also linear (e.g., Businger 1982). The elemental solution for surface emission (deposition) required in (1) is that for a unit surface point source (sink). For the special case of a surface point source with an emission rate Q, $F_0(x', y') = Q\delta(x')\delta(y')$ and substitution in (1) gives

$$f(x, y, z_m) = \frac{F_m(x, y, z_m)}{Q}, \tag{2}$$

that is, the flux footprint is equal to the vertical flux downwind of a unit surface point source.

Horst and Weil (1992) showed that, within the surface flux layer, the dependence of the flux footprint on crosswind location is identical to the crosswind concentration distribution downwind of a surface point source. The crosswind-integrated footprint $\bar{f}^y$ is equal to the crosswind-integrated flux downwind of a unit surface point source. Integrating the two-dimensional advection–diffusion equation from the surface to height z_m, HW found that

$$\bar{f}^y(x, z_m) \equiv \int_{-\infty}^{\infty} f(x, y, z_m)dy \tag{3}$$

$$= -\frac{\partial}{\partial x}\int_0^{z_m} \bar{u}(z)\frac{\bar{C}^y(x, z)}{Q}dz, \tag{4}$$

where $\bar{u}(z)$ is the mean wind speed profile and $\bar{C}^y$ is the crosswind-integrated concentration distribution downwind of a surface point source Q.

In the following, section 2 summarizes the HW flux footprint model that is the basis for the analysis of this paper, section 3 discusses the streamwise and crosswind dimensions of the flux footprint, section 4 presents the fetch requirements for flux measurement, and section 5 discusses the conditions in which these results may be applied, in particular for near-surface flux measurement in a convective boundary layer. The appendix presents analytic solutions and approximations that may be used for estimation of the flux footprint.

2. Footprint model

Horst and Weil (1992) used both analytic and Lagrangian stochastic dispersion models to estimate $\bar{C}^y/Q$ and calculate the crosswind-integrated flux footprint. The analytic model for the crosswind-integrated concentration distribution is (van Ulden 1978; Horst 1979)

$$\frac{\bar{C}^y(x, z)}{Q} = \frac{A}{\bar{z}U}e^{-(z/b\bar{z})^r}, \tag{5}$$

where $A = r\Gamma(2/r)/\Gamma^2(1/r)$, $b = \Gamma(1/r)/\Gamma(2/r)$, Γ is the gamma function, $\bar{z}$ is the mean plume height for dispersion from a surface source,

$$\bar{z}(x) \equiv \frac{\int_0^{\infty} z\bar{C}^y(x, z)dz}{\int_0^{\infty} \bar{C}^y(x, z)dz}, \tag{6}$$

and U is the plume advection velocity,

$$U(x) \equiv \frac{\int_0^{\infty} \bar{u}(z)\bar{C}^y(x, z)dz}{\int_0^{\infty} \bar{C}^y(x, z)dz}. \tag{7}$$

Observations of vertical profiles downwind of a surface source suggest that $1 \leqslant r \leqslant 2$, depending on atmospheric stability (Elliot 1961; Nieuwstadt and van Ulden 1978; Pasquill and Smith 1983). Here, $\bar{z}$ is calculated from the Lagrangian similarity equation (van Ulden 1978),

$$\frac{d\bar{z}}{dx} = \frac{k^2}{[\ln(p\bar{z}/z_0) - \psi_m(p\bar{z}/L)]\phi_h(p\bar{z}/L)}. \tag{8}$$

Here, $p \approx 1.55$, $k = 0.4$ is the von Kármán constant, z_0 is the surface roughness length, L is the Obukhov length, and ψ_m and ϕ_h are the common surface-flux-layer functions that describe the dependence on atmospheric stability of the wind profile and the eddy diffusivity for sensible heat (see appendix). From (8) we find that $x \approx \bar{z}\ln(\bar{z}/z_0)$ for neutral conditions ($\bar{z}/L = 0$, $\psi_m = 0$, $\phi_h = 1$); $\bar{z}$ increases more rapidly with x for unstable conditions ($\bar{z}/L < 0$, $\psi_m > 0$, $\phi_h < 1$); and $\bar{z}$ increases less rapidly with x for stable conditions ($\bar{z}/L > 0$, $\psi_m < 0$, $\phi_h > 1$). An analytic solution

of (8) for $x(\bar{z})$, as well as approximate analytic solutions of (4) for $\bar{f}^y$ and (7) for $U(x)$, are found in the appendix.

The analytic diffusion model assumes a self-similar form for the vertical concentration profile [Eq. (5)]. Although this is found to provide a good match to observations, the relevant field data are somewhat limited. To examine the validity of this simplifying assumption, HW used a Lagrangian stochastic diffusion model that calculates random particle trajectories from equations for the rates of change of particle height z_p and streamwise displacement x_p,

$$\frac{dz_p}{dt} = w_L[z_p(t), t], \quad \frac{dx_p}{dt} = \bar{u}[z_p(t)]. \qquad (9)$$

The rate of change of Lagrangian vertical velocity w_L has both deterministic and stochastic forcing terms that are functions of the Eulerian turbulent flow field. For simplicity, horizontal velocity fluctuations are ignored, and thus the streamwise displacement is assumed to depend simply on the mean wind speed profile. The concentration profile is found from a probability density function of particle height that is evaluated numerically from the particle trajectories.

Based on the functional form of $\bar{f}^y$ predicted by the analytic model, HW proposed a normalized crosswind-integrated footprint,

$$\Phi \equiv \frac{z_m \bar{f}^y(x, z_m)}{d\bar{z}/dx}. \qquad (10)$$

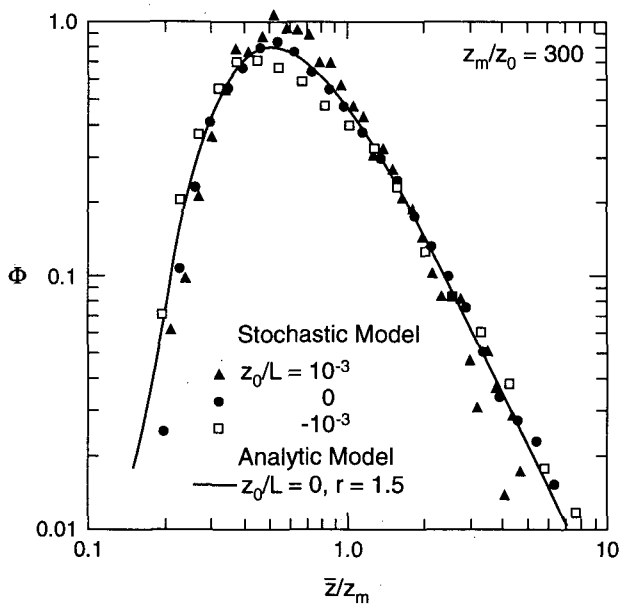

FIG. 2. Stochastic model estimates of $\Phi(\bar{z}/z_m)$ for $z_m/z_0 = 300$ and $z_0/L = 0, \pm 10^{-3}$, compared with the analytic model estimate for $z_0/L = 0$, $r = 1.5$.

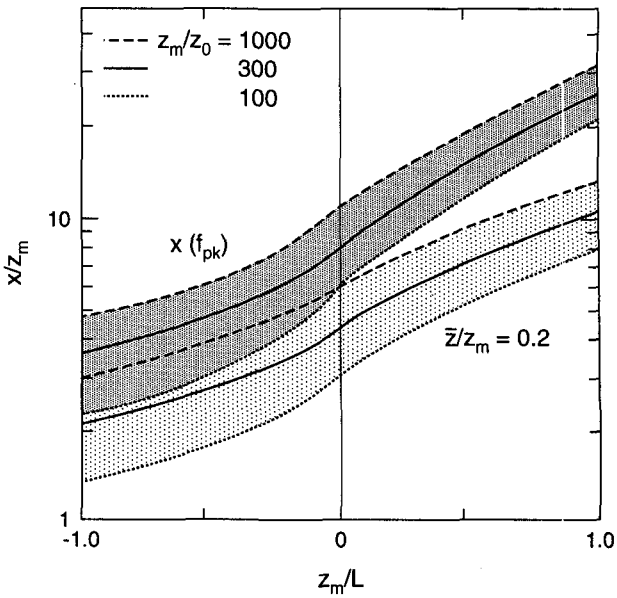

FIG. 3. Normalized location x/z_m of the peak of f and of the point where $\bar{z}/z_m = 0.2$, as a function of z_m/L for $z_m/z_0 = 100$, 300, and 1000.

They demonstrated that Φ depends principally on the single variable $\bar{z}/z_m$, and that the explicit dependence of $\bar{f}^y$ on downwind distance, thermal stability, and surface roughness is then contained in the dependence of $\bar{z}$ on these variables. Figure 2 compares Lagrangian stochastic model estimates of Φ for $z_m/z_0 = 300$ and $z_0/L = 0, \pm 10^{-3}$ with the analytic model estimate for $z_0/L = 0$, $r = 1.5$. The dependence of Φ on atmospheric stability is weak, and the analytic curve for neutral stability provides a reasonable overall fit to the stochastic model estimates. The good agreement between the analytic and stochastic models seen in Fig. 2 (and Fig. 4) demonstrates that the vertical concentration profiles do not depart to a significant degree from the self-similar form assumed by the analytic model.

3. The dimensions of the flux footprint

The measured flux is essentially unaffected by a change in the surface flux that occurs directly below the flux sensor or in a limited region immediately upwind of the sensor. The upwind extent of this region of minimal influence can be determined from Fig. 2, where we see that the contribution to the measured flux is very small for $\bar{z}/z_m < 0.2$. This region makes a contribution, per unit surface flux, of less than 1% to the measured flux. Using (8) to transform from $\bar{z}/z_m$ to x/z_m (see appendix), the distance from the measurement location to the point at which $\bar{z}/z_m = 0.2$ is shown explicitly in Fig. 3 as a function of z_m/L. Separate curves are shown for $z_m/z_0 = 100$, 300, and 1000. For neutral stability, this nearby boundary of the foot-

print is at an upwind distance equal to 3–6 times the measurement height, but this distance can range from less than 2 times the measurement height for unstable conditions to more than 10 times the measurement height for stable conditions. Note that for a variation of z_m/z_0 by a factor of 10, x/z_m varies by a factor of 2 or less. Thus these results are not very sensitive to z_m/z_0 and the scaling of x and L with z_m provides estimates that are roughly self-similar.

It can be seen from Fig. 2 that for neutral stability the peak of the nondimensional crosswind-integrated footprint Φ occurs at $\bar{z}/z_m \approx 0.5$. However, the location of the peak of the crosswind-integrated footprint, $\bar{f}^y = (\Phi/z_m)d\bar{z}/dx$, varies from $\bar{z}/z_m \approx 0.55$ in strongly unstable conditions ($\partial^2\bar{z}/\partial x^2 > 0$) to $\bar{z}/z_m \approx 0.4$ in strongly stable conditions ($\partial^2\bar{z}/\partial x^2 < 0$). Because the crosswind width of the footprint increases with x, the peak of the three-dimensional footprint function $f(x, y, z_m)$ occurs closer to the measurement location than the peak of the crosswind-integrated footprint; about 20% closer if we assume that, for the short distances being considered, the crosswind width is a linear function of x. In Fig. 3 we see that for neutral stability the normalized location of the peak of the footprint, $x(f_{pk})/z_m$, occurs at an upwind distance equal to 6–10 times the measurement height, but for diabatic conditions this distance can range from less than 3 to over 30 times the measurement height. These results are equivalent to those presented in dimensional form by Leclerc and Thurtell (1990) for the crosswind-integrated footprint.

The crosswind extent of the footprint can be estimated directly from the crosswind width of the plume from a surface point source. Near the source, it is found that $\sigma_y \sim x\sigma_\theta$, where σ_y^2 and σ_θ^2 are the variances of the crosswind concentration distribution and the wind direction distribution (e.g., Doran et al. 1978). A quantitative estimate of the plume width is provided, for example, by Briggs, who has combined data from several atmospheric diffusion experiments to estimate σ_y near the source ($x < 1$–2 km) to be $0.22x$, $0.08x$, and $0.04x$ for very unstable, neutral, and very stable conditions, respectively (Hanna 1982).

4. Fetch requirements for flux measurement

In the alongwind direction, a commonly used rule of thumb is that measurement of a surface flux by micrometeorological techniques requires a uniform upwind fetch equal to 100 times the measurement height (Businger 1986). Leclerc and Thurtell (1990), however, note from their Lagrangian stochastic model estimates of the flux footprint that this rule underestimates fetch requirements when observations are made above smooth surfaces, in stable conditions, or at large measurement heights. The upwind extent of the flux footprint can be quantified by considering the special case of a uniform surface flux S_0 that has an unlimited extent in the crosswind direction, but extends for only a finite distance x_0 upwind of the measurement location,

$$F_0(s) = \begin{cases} 0, & s > x_0 \\ S_0, & s \leq x_0, \end{cases} \tag{11}$$

where $s \equiv x - x'$. Crosswind integrating (1) over all y and substituting from (10) and (11),

$$F_m(x_0) = \int_0^{x_0} S_0 \bar{f}^y(s, z_m)ds, \tag{12}$$

$$= S_0 \int_0^{x_0} \frac{\partial(\bar{z}/z_m)}{\partial s} \Phi\left(\frac{\bar{z}}{z_m}\right)ds, \tag{13}$$

$$= S_0 \int_0^{\zeta(x_0)} \Phi(\zeta')d\zeta', \quad \zeta \equiv \frac{\bar{z}}{z_m}, \tag{14}$$

where $\bar{z} = \bar{z}(s)$. The ratio of the measured flux to the surface flux is equal to the streamwise integral of the crosswind-integrated footprint.

Figure 4 shows $F_m/S_0 = \int_0^{\zeta(x_0)} \Phi(\zeta')d\zeta' \equiv F/S_0$ as a function of $\bar{z}(x_0)/z_m$ for $z_m/z_0 = 300$ and a range of atmospheric stability. Note that there is a weak residual dependence of F/S_0 on atmospheric stability. This figure compares Lagrangian stochastic model estimates with analytic model estimates for three values of the exponent r. There is good agreement between the analytic and stochastic model estimates, particularly for the neutral and stable cases. The stochastic model results suggest that r is equal to 2 for stable conditions, 1.5 for neutral conditions, and about 1 for unstable conditions. These exponents are in agreement with field

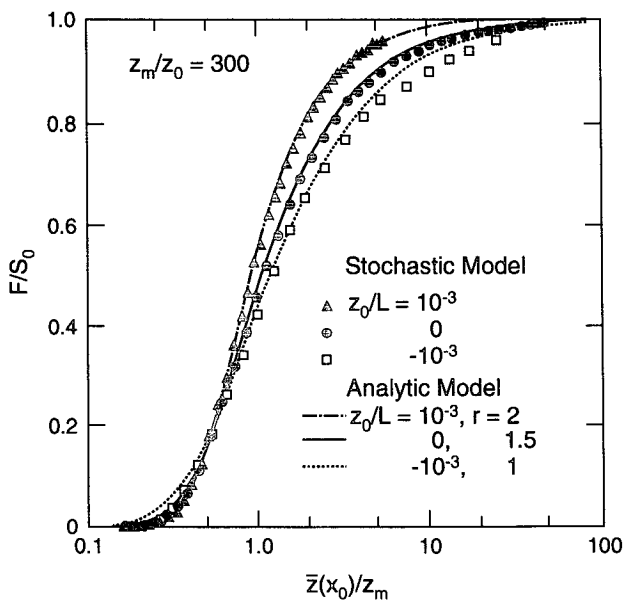

FIG. 4. Normalized vertical flux F/S_0 as a function of $\bar{z}(x_0)/z_m$ for $z_m/z_0 = 300$ and a range of atmospheric stability.

observations of vertical concentration profiles downwind of a surface source (Elliot 1961; Nieuwstadt and van Ulden 1978).

Note again that the measured flux is relatively unaffected by the surface flux in the immediate vicinity of the measurement site, that is, for $\bar{z}/z_m \leq 0.2$. At the other extreme, the measured flux is essentially equal to the surface flux ($F/S_0 \rightarrow 1$) for $\bar{z}/z_m$ between 20 and 100, depending on stability. Figure 5 shows the upwind fetch required for the measured flux to be within specified fractional errors, $1 - F/S_0$, of the surface flux, where the fetch is again normalized with the measurement height and plotted as a function of z_m/L. Normalized fetches are shown for $z_m/z_0 = 300$ and a range of fractional errors. To demonstrate that the scaling of x_0 and L with z_m again provides estimates that are roughly self-similar, fetches also are shown for $100 \leq z_m/z_0 \leq 1000$ and a fractional error of 0.10 (shaded area). It can be seen from Fig. 5 that for many situations the measured flux is within 10%–20% of the surface flux only if the fetch is considerably greater than 100 times the measurement height. The required fetch is strongly dependent on atmospheric stability; stable conditions require a much greater fetch than do unstable conditions, and the fetch required for even moderately stable conditions is surprisingly large.

However, the results shown in Fig. 5 are for the simple case where the surface flux is equal to zero upwind of x_0. Rather than assume that there is no emission or deposition upwind of x_0, we can more generally specify a step change in the surface flux,

$$F_0(s) = \begin{cases} S_1, & s > x_0 \\ S_2, & s \leq x_0. \end{cases} \tag{15}$$

The flux measured downwind of a general step change in the surface flux can be determined from Eq. (14) by using linear superposition:

$$F_m(x_0) = S_1 \int_0^\infty \Phi(\zeta')d\zeta' + (S_2 - S_1) \int_0^{\zeta(x_0)} \Phi(\zeta')d\zeta' \tag{16}$$

$$= S_1 + (S_2 - S_1)\frac{F}{S_0}. \tag{17}$$

Recall that as $x_0 \rightarrow 0$, $F/S_0 \rightarrow 0$ and thus the measured flux will approach S_1, while as $x_0 \rightarrow \infty$, $F/S_0 \rightarrow 1$ and the measured flux will approach S_2. This superposition technique can be extended to any number of streamwise step changes, but (1) must be used directly for the more general case of a two-dimensional distribution of surface flux.

Solving (17) for the fractional error in the measurement of the local surface flux, $1 - [F_m(x_0)/S_2]$, provides a relation that enables direct use of Fig. 5 for the case of a general step change,

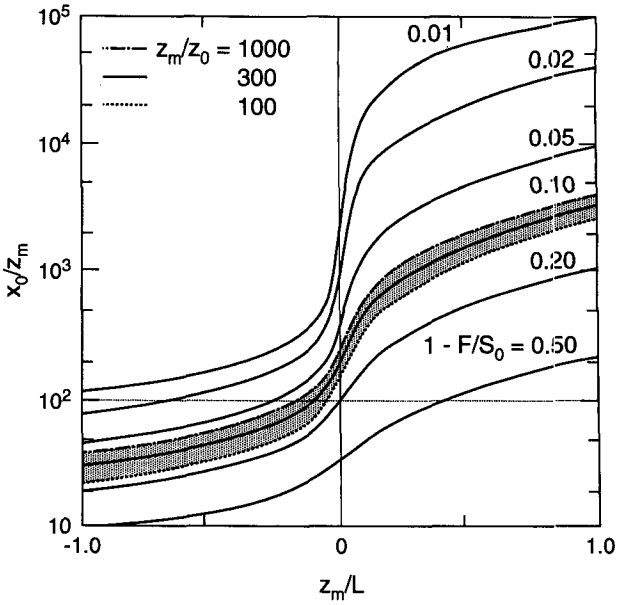

FIG. 5. Normalized fetch x_0/z_m required for the measured flux to be within specified fractions of the surface flux, as a function of z_m/L and z_m/z_0.

$$1 - \frac{F_m(x_0)}{S_2} = \left(1 - \frac{S_1}{S_2}\right)\left(1 - \frac{F}{S_0}\right). \tag{18}$$

Given the fetch, measurement height, and atmospheric stability, we can determine a value for $1 - (F/S_0)$ from Fig. 5 and then multiply by $1 - (S_1/S_2)$ to determine the corresponding fractional error in the more general case. (Note that if $S_1 < S_2$, then $F_m < S_2$ and the fractional error is positive and if $S_1 > S_2$, then $F_m > S_2$ and the fractional error is negative.) Thus if the ratio of the upwind surface flux to the local surface flux, S_1/S_2, is equal to either 0 or 2, the absolute value of the fractional error is identical to that in Fig. 5; if S_1/S_2 is between 0 and 2, the absolute value of the fractional error is less than that of Fig. 5; and if S_1/S_2 is less than 0 or greater than 2, the absolute value of the fractional error is greater than that of Fig. 5.

5. Discussion

These fetch estimates are based principally on an analytic vertical dispersion model that has been verified by comparison with field observations (van Ulden 1978; Horst 1979; Pasquill and Smith 1983) and by comparison with a numerical Lagrangian stochastic dispersion model (HW). The latter comparison supports the validity of both the analytic and numerical models, because the only overlap between the two models is their use of a common empirical description of the surface-flux-layer flow field. However, several simplifying assumptions have been made to obtain the results shown in Fig. 5. Two basic, implicit assumptions

are conservation of the quantity whose flux is being investigated and steady state of both the surface flux and the turbulent flow field. More restrictive assumptions are horizontal homogeneity of the turbulent flow field and that the measurement height must be less than the depth of the atmospheric surface layer.

The assumption that the turbulent flow field is horizontally homogeneous effectively limits these results to fluxes of passive scalars, that is, those that do not affect the flow field. The present flux footprint model also quantifies the spatial distribution of the upwind surface contributions to the flux of a nonpassive scalar, such as sensible heat, provided that the surface flux is a priori constrained to be uniform in order to maintain a horizontally homogeneous turbulence field. Thus for nonpassive scalars, the applications of the present footprint function are very limited.

The use of empirical atmospheric–surface-layer relations for $\bar{u}$ and ϕ_h [cf. (4), (7), and (8)] formally limits these results to circumstances where both z_m and $\bar{z}$ are less than the depth of the surface layer. (However, the surface-layer relations may be usefully valid at heights exceeding the depth of the surface layer.) The restriction on $\bar{z}$ will often be the most limiting, particularly for consideration of questions of adequate fetch, and may be a quite serious restriction when we are interested in cases with $\bar{z}/z_m > 10$, as is required for $F/S_0 \to 1$. The present model effectively assumes that the surface-layer depth is unlimited or that z_m and $\bar{z}$ are both a small fraction of the boundary layer depth, so that $F/S_0 \to 1$ for $\bar{z}/z_m \gg 1$; that is, as $x \to \infty$, there is a negligibly small divergence of the vertical flux within the layer $z \leqslant z_m$.

When $\bar{z}/z_m \gg 1$, vertical diffusion is less likely to be limited to the surface layer and thus may be influenced by processes occurring throughout the boundary layer. Weil and Horst (1992) investigated the flux footprint for the convective boundary layer (CBL), assuming that the entrainment flux at the top of the boundary layer was equal to zero. They found that, for a large fetch, F/S_0 approached an equilibrium value that was less than unity and equal to $1 - (z_m/h)$, where h is the depth of the boundary layer. This result is consistent with the common assumption that the flux profile is linear in a well-mixed, horizontally homogeneous boundary layer (Wyngaard 1984). In the more general case, the measured flux is also a function of the entrainment flux F_e,

$$F_m = S_0 + \frac{z_m}{h}(F_e - S_0), \tag{19}$$

where S_0 is again the flux at the surface. Thus F_m/S_0 approaches unity in the limit of a large uniform fetch only if $F_e = S_0$ or $z_m/h \ll |S_0/(F_e - S_0)|$. Therefore, it might be reasonable to surmise that the fetch estimates for the unlimited surface flux layer (Fig. 5) are a lower limit for the fetches required in a real atmospheric boundary layer (with $F_e = 0$).

This latter hypothesis can be examined for the CBL by calculating near-surface fetches using the values of F/S_0 estimated by Weil and Horst (1992). As noted above, the CBL predictions approach an equilibrium value of $F/S_0 = 1 - (z_m/h)$. However, F/S_0 overshoots its equilibrium value and first equals $1 - (z_m/h)$ at a normalized downwind distance that we will denote as $X = X_0$. Here $X \equiv w_* x/Vh$, where $w_* = u_*(h/k|L|)^{1/3}$ is the convective velocity scale, u_* is the friction velocity, and V is the mean CBL wind speed, approximated by Garratt et al. (1982) as $V \approx (u_*/k)[\ln(0.1h/z_0) - \ln|h/L|^{1/2}]$. The CBL fetches can be compared to those for the unlimited surface layer by normalizing the CBL fetches as in Fig. 5,

$$\frac{x_0}{z_m} = \frac{k^{1/3}(V/u_*)X_0}{(z_m/h)^{2/3}|z_m/L|^{1/3}}. \tag{20}$$

Note, however, that because the CBL fluxes approach an equilibrium value that is not equal to S_0, the basis on which to compare the two models is ambiguous. For the CBL fetches, a fractional error defined in terms of the equilibrium flux, $1 - F\{S_0[1 - (z_m/h)]\}^{-1}$, is smaller than a fractional error defined in terms of the surface flux, $1 - (F/S_0)$, while for the unlimited surface-layer fetch estimates ($z_m/h \to 0$) the two definitions are identical.

Figure 6 compares normalized CBL and unstable surface-layer fetches for $z_m/z_0 = 10^3$; CBL fetch estimates are shown for $z_m/h = 0.05$ and 0.10. To directly address the primary subject of this study, the fractional errors in Fig. 6 are calculated on the basis of the surface flux: $1 - (F/S_0) = 0.05$, 0.1, 0.2, and 0.5 for $z_m/h = 0.05$ and $1 - (F/S_0) = 0.1$, 0.2, and 0.5 for $z_m/h = 0.10$. In this figure we have extended the surface-

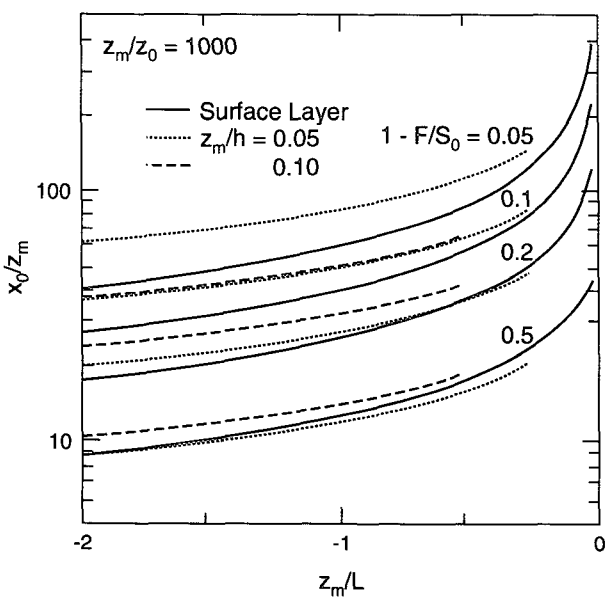

FIG. 6. Normalized fetch x_0/z_m, as in Fig. 5, for the unlimited surface-layer model and for the CBL model ($z_m/h = 0.05$ and 0.10).

layer fetch estimates to $z_m/|L| = 2$ in order to compare to CBL fetch estimates for $h/|L| \to 40$ ($z_m/h = 0.05$) and $h/|L| \to 20$ ($z_m/h = 0.10$). Although the model used in the CBL simulation is formally valid only for $h/|L| > 10$, the CBL fetch estimates are plotted for $h/|L| > 5$. The best agreement between the fetches estimated by the two models is found for moderately unstable conditions (and in fact the agreement continues to improve for $h/|L| < 5$). For strongly unstable conditions, the CBL fetch estimates exceed those for the surface layer, but for $z_m/|L| < 2$ they are still within a factor of two of the surface-layer fetches.

If, on the other hand, we define the fractional error on the basis of the equilibrium flux, the CBL fetches shown in Fig. 6 correspond to fractional errors of 0, 0.05, 0.16, and 0.47 for $z_m/h = 0.05$ and 0, 0.11, and 0.44 for $z_m/h = 0.10$. In that case the CBL fetch estimates are smaller than those for the surface layer, but again the fetch estimates from the two models agree within a factor of less than two (with the exception of the CBL curves for a fractional error of zero, for which the surface-layer model requires an infinite fetch). Thus, with either definition of the fractional error, the agreement between the two models is reasonably good, particularly in view of the lack of a resolved surface layer in the CBL model and the limited overlap in their formal ranges of validity in z_m/L. In particular we find that, when we define the fractional error in terms of the local surface flux, the fetch estimates for the CBL equal or exceed those for the unlimited surface layer, as was surmised above.

Acknowledgments. The authors are grateful for helpful discussions of this research with our colleagues, Don Lenschow, Steve Oncley, and Leif Kristensen, and for the insightful review comments of John Wyngaard.

APPENDIX

Analytic Formulas for $\bar{f}^y$, $\bar{z}$, U, and F/S_0

Even with the analytic diffusion model [Eqs. (5)–(8)] calculation of $\bar{f}^y$ or Φ with a realistic wind profile requires numerical evaluation of the integral in (4). Consequently, HW suggested empirical formulas for Φ that were obtained by parametric fits to the analytic and stochastic model estimates. However, a better approximation is found by changing the variable of integration in (4) to $\xi \equiv z/\bar{z}$ and using the chain rule to transform the derivative with respect to x to a derivative with respect to $\bar{z}$,

$$\bar{f}^y = -\frac{d\bar{z}}{dx}\frac{\partial}{\partial \bar{z}}\int_0^{z_m/\bar{z}} \frac{\bar{u}(\xi\bar{z})}{U} A e^{-(\xi/b)^r} d\xi. \quad \text{(A1)}$$

Noting that $U \approx \bar{u}(c\bar{z})$ (see below) leads to the speculation that the integrand is principally a function of ξ and is insensitive to $\bar{z}$. With this assumption, Leibnitz's rule for differentiation of an integral with respect to a parameter gives

$$\bar{f}^y \approx -\frac{d\bar{z}}{dx}\frac{\partial}{\partial \bar{z}}\left(\frac{z_m}{\bar{z}}\right)\left[\frac{\bar{u}(\xi\bar{z})}{U(\bar{z})} A e^{-(\xi/b)^r}\right]_{\xi = z_m/\bar{z}}, \quad \text{(A2)}$$

and thus,

$$\Phi \equiv \frac{z_m \bar{f}^y(x, z_m)}{d\bar{z}/dx} \approx \left(\frac{z_m}{\bar{z}}\right)^2 \frac{\bar{u}(\bar{z}_m)}{U(\bar{z})} A e^{-(z_m/b\bar{z})^r}. \quad \text{(A3)}$$

For $z_0/L \leq 0$, the error in this approximation is generally an overestimation of Φ by about 5%, while for $z_0/L > 0$, the error is an underestimation by less than 5% near the peak that increases to 10%–20% as Φ decreases to 0.01 at large values of $\bar{z}/z_m$.

To evaluate Φ we need to also know $\bar{z}(x)$ and $U(\bar{z})$, defined in (6) and (7). Here, $\bar{z}(x)$ [actually, $x(\bar{z})$] is found by integrating (8) using the Businger–Dyer formulas for ϕ_h and ψ_m. For $\bar{z}$ ($x = 0$) $= z_0$,

$$\frac{x}{z_0} = \int_{z_0}^{\bar{z}(x)} \left(\frac{\partial \bar{z}'}{\partial x}\right)^{-1} d\bar{z}' \equiv \Psi(\bar{z}) - \Psi(z_0), \quad \text{(A4)}$$

where for $z_0/L \geq 0$,

$$\phi_h \equiv \frac{u_* k z}{K_h} = \left(1 + \frac{\beta z}{L}\right), \quad \text{(A5)}$$

$$\psi_m \equiv \ln\left(\frac{z}{z_0}\right) - \frac{k\bar{u}}{u_*} = -\frac{\beta z}{L}, \quad \text{(A6)}$$

$$\Psi(\bar{z}) = \frac{1}{k^2}\frac{\bar{z}}{z_0}\left\{\ln\left(\frac{p\bar{z}}{z_0}\right) - 1 + \frac{\beta p\bar{z}}{L}\left[\frac{1}{4} + \frac{\beta p\bar{z}}{3L} + \frac{1}{2}\ln\left(\frac{p\bar{z}}{z_0}\right)\right]\right\}. \quad \text{(A7)}$$

Here K_h is the eddy diffusivity for sensible heat. Dyer (1974) suggests $\beta = 5$, $k = 0.41$. Other sources suggest a different value of β for ϕ_h than for ψ_m (e.g., Högström 1988), but it is a simple matter to integrate (8) for this case also. For $z_0/L < 0$,

$$\phi_h = \left(1 - \frac{\gamma z}{L}\right)^{-1/2}, \quad \text{(A8)}$$

$$\psi_m = 2\ln\left(\frac{y+1}{2}\right) + \ln\left(\frac{y^2+1}{2}\right) + 2\tan^{-1}\left(\frac{1-y}{1+y}\right), \quad \text{(A9)}$$

$$y \equiv \frac{1}{\varphi_m} = \left(1 - \frac{\gamma z}{L}\right)^{1/4},$$

$$\Psi(\bar{z}) = \frac{1}{k^2}\frac{2|L|}{\gamma p z_0}\left\{2(y_p^2+1)\tan^{-1}(y_p) - (y_p^2-1)\ln\left(\frac{y_p+1}{y_p-1}\right) - 4y_p + y_p^2\left[3\ln(2) - \frac{\pi}{2} - \ln\left(\frac{\gamma p z_0}{|L|}\right)\right]\right\},$$

$$y_p \equiv \left(1 - \frac{\gamma p\bar{z}}{L}\right)^{1/4}. \quad \text{(A10)}$$

Dyer (1974) suggests $\gamma = 16$. Again, other sources suggest different values of γ for ϕ_h and φ_m, but we can integrate (8) analytically only for the special case where $\phi_h = \phi_m^2$. [The latter condition follows identically from the assumption Ri $= z/L$, where Ri is the gradient Richardson number, and this is observed to be a good approximation in the unstable surface layer (Businger 1988).]

For a logarithmic wind profile and the analytic dispersion model [Eq. (5)] $U = \bar{u}(c\bar{z})$, where

$$c = b \exp\left[Ab \int_0^\infty \ln(y) e^{-y^r} dy \right]. \quad \text{(A11)}$$

Horst (1979) evaluated this integral numerically and found $c = 0.66$ for $r = 2$, 0.63 for $r = 1.5$, and 0.56 for $r = 1$. In the more general case of a diabatic wind profile, van Ulden (1978) finds that

$$U\left(\bar{z}, \frac{z_0}{L} \geq 0\right) = \frac{u_*}{k}\left[\ln\left(\frac{c\bar{z}}{z_0}\right) + \frac{\beta\bar{z}}{L}\right], \quad \text{(A12)}$$

$$U\left(\bar{z}, \frac{z_0}{L} < 0\right) \approx \frac{u_*}{k}\left[\ln\left(\frac{c\bar{z}}{z_0}\right) - \psi_m\left(\frac{c\bar{z}}{L}\right)\right]. \quad \text{(A13)}$$

Note that (A11) is strictly valid only for $z_0/L \geq 0$. However, for all stabilities, the values for $c(r)$ calculated with (A11) give better agreement with a numerical evaluation of (7) than the generic value 0.6 suggested by van Ulden. Note also that for stable conditions, $U \neq \bar{u}(c\bar{z})$. This is likely the reason why our approximation for Φ [Eq. (A3)] is less satisfactory in stable conditions.

Finally, F/S_0 is calculated from (12) or (14). We have not been able to evaluate these integrals analytically with realistic wind profiles. However, for the special case of a uniform wind profile,

$$\frac{F}{S_0} = 1 - \frac{1}{\Gamma(1/r)} \int_0^{t_0} e^{-t} t^{(r^{-1}-1)} dt, \quad t_0 \equiv \left[\frac{z_m}{b\bar{z}(x_0)}\right]^r, \quad \text{(A14)}$$

$$= 1 - \frac{\gamma(1/r, t_0)}{\Gamma(1/r)}, \quad \text{(A15)}$$

$$= \begin{cases} e^{-z_m/\bar{z}}, & r = 1 \\ 1 - \operatorname{erf}(z_m/\pi^{1/2}\bar{z}), & r = 2, \end{cases} \quad \text{(A16)}$$

where $\gamma(1/r, t_0)$ is the incomplete gamma function.

REFERENCES

Businger, J. A., 1982: Equations and concepts. *Atmospheric Turbulence and Air Pollution Modelling,* F. T. M. Nieuwstadt and H. van Dop, Eds., D. Reidel, 1–36.

——, 1986: Evaluation of the accuracy with which dry deposition can be measured with current micrometeorological techniques. *J. Climate Appl. Meteor.,* **25,** 1100–124.

——, 1988: A note on the Businger–Dyer profiles. *Bound.-Layer Meteor.,* **42,** 145–151.

Doran, J. C., T. W. Horst, and P. W. Nickola, 1978: Variations in measured values of lateral diffusion parameter. *J. Appl. Meteor.,* **17,** 825–831.

Dyer, A. J., 1974: A review of flux-profile relationships. *Bound.-Layer Meteor.,* **7,** 363–372.

Elliot, W. P., 1961: The vertical diffusion of gas from a continuous source. *Int. J. Air Water Pollut.,* **4,** 33–46.

Garratt, J. R., J. C. Wyngaard, and R. J. Francey, 1982: Winds in the atmospheric boundary layer—Prediction and observation. *J. Atmos. Sci.,* **39,** 1307–1316.

Hanna, S. R., 1982: Applications in air pollution modeling. *Atmospheric Turbulence and Air Pollution Modelling,* F. T. M. Nieuwstadt and H. van Dop, Eds., D. Reidel, 275–310.

Högström, U., 1988: Non-dimensional wind and temperature profiles in the atmospheric surface layer: A reevaluation. *Bound.-Layer Meteor.,* **42,** 55–78.

Horst, T. W., 1979: Lagrangian similarity modeling of vertical diffusion from a ground-level source. *J. Appl. Meteor.,* **18,** 733–740.

——, and J. C. Weil, 1992: Footprint estimation for scalar flux measurements in the atmospheric surface layer. *Bound.-Layer Meteor.,* **59,** 279–296.

Leclerc, M. Y., and G. W. Thurtell, 1990: Footprint predictions of scalar fluxes using a Markovian analysis. *Bound.-Layer Meteor.,* **52,** 247–258.

Nieuwstadt, F. T. M., and A. P. van Ulden, 1978: A numerical study on the vertical dispersion of passive contaminants from a continuous source in the atmospheric surface layer. *Atmos. Environ.,* **12,** 2119–2124.

Pasquill, F., and F. B. Smith, 1983: *Atmospheric Diffusion.* 3d ed. John Wiley and Sons.

Schuepp, P. H., M. Y. Leclerc, J. I. MacPherson, and R. L. Desjardins, 1990: Footprint prediction of scalar fluxes from analytical solutions of the diffusion equation. *Bound.-Layer Meteor.,* **50,** 355–373.

van Ulden, A. P., 1978: Simple estimates for vertical diffusion from sources near the ground. *Atmos. Environ.,* **12,** 2125–2129.

Weil, J. C., and T. W. Horst, 1992: Footprint estimates for atmospheric flux measurements in the convective boundary layer. *Precipitation Scavenging and Atmosphere–Surface Exchange,* Vol. 2, S. E. Schwartz and W. G. N. Slinn, Eds., Hemisphere Publishing, 717–728.

Wyngaard, J. C., 1984: Toward convective boundary layer parameterizations: A scalar transport module. *J. Atmos. Sci.,* **41,** 1959–1969.